

Parameterization of Snow Albedo for Climate Models

Susan Marshall
Department of Geography
University of Colorado
Boulder, Colorado, U.S.A.

Stephen G. Warren
Department of Atmospheric Sciences
University of Washington
Seattle, Washington, U.S.A.

Abstract

General circulation models (GCMs) find that the response of climate to increases in CO₂ is enhanced by the snow-albedo-temperature feedback. The results are very sensitive to the assumed value of snow albedo. Snow albedo, however, is highly variable, and it is not calculated accurately in present-day GCMs. We would like to replace the current simple empirical parameterizations of snow albedo with a physically-based parameterization which is accurate yet efficient to compute.

Our approach is to develop simple functions which fit the spectrally-averaged results of a detailed theoretical model of the spectral albedo of snow which uses the delta-Eddington method for multiple scattering and Mie theory for single scattering. The spectrally-averaged snow albedo varies with snow grain size, solar zenith angle, snow cover thickness, underlying surface albedo (for thin snow), concentration of absorptive impurities in the snowpack, and cloud optical thickness (because clouds alter the solar spectrum at the surface). This method divides the solar spectrum into the two broad wavebands commonly used in climate models: visible and near-infrared.

General circulation models (GCMs) find that the response of climate to increases in CO₂ is enhanced by the snow-albedo-temperature feedback. The results are sensitive to the assumed value of snow albedo. Snow albedo, however, is highly variable, and it is not calculated accurately in present-day GCMs. Most GCMs assign a single value to the albedo of an optically-thick snow cover. These albedo values can range from 0.55 to 0.85, and generally remain constant with time until the snowpack decays to some critical depth, then decrease as a function of the snow depth until the albedo reaches the underlying surface albedo. Other GCMs allow the snow albedo to vary with solar zenith angle, snowpack thickness, age of the snow layer, and latitude. We would like to replace the current simple empirical parameterizations of snow albedo with a physically-based parameterization which is accurate yet efficient to compute.

Our approach is to develop simple functions which fit the spectrally-averaged results of a detailed theoretical model of the spectral albedo of snow which uses the delta-Eddington method for multiple scattering and Mie theory for single scattering (Wiscombe and Warren, 1980, Warren and Wiscombe, 1980, hereafter WWI and WWII, respectively). This method assumes a homogeneous snow-covered surface with no vegetation cover. The GCMs we surveyed (NCAR, GFDL, OSU, GISS, GLAS, LMD, UKMO, and ECMWF) break the solar spectrum into at most two parts. The break is either at 0.7 μm or 0.9 μm wavelength) with one exception at 0.78 μm). We therefore also break the solar spectrum into two parts, "visible" and "near-infrared" (NIR). We will develop the parameterizations for the two regions split at 0.7 μm . Then we expect that the functional forms we develop can also be used when the break is at 0.9 μm , so we will need only to develop a second set of coefficients for those climate models which break the spectrum at 0.9 μm . In all examples given here, the separation between "visible" and "near-infrared" is at 0.7 μm .

The spectrally-averaged snow albedo varies directly with snow grain radius, r , effective solar zenith angle, θ , snow cover thickness, h (g cm^{-2}), underlying surface albedo (for thin snow), u_a , and concentration of absorptive impurities (especially soot) in the snow layer, s ; and indirectly with cloud cover. Figure 1 shows the effects of snow grain size and zenith angle on the spectral albedo of snow to be much greater in NIR wavelengths, while the effects of finite snow thickness and soot concentration on the spectral albedo are greater in the visible wavelengths. The similarity between the spectral signatures of grain size and zenith angle, and those of snowpack thickness and soot concentration, suggest that each pair of variables might be lumped together as one predictor.

The predictors of snow albedo will be effective grain size, r , effective zenith angle, θ , (which will depend on the diffuse direct ratio), impurity content, s , (as an effective soot content), and snowpack thickness, h (g cm^{-2}). In the NIR there will be an additional predictor, the atmospheric transmittance, t . This is needed because snow albedo varies greatly with wavelength, and the absorption of solar radiation by clouds is also wavelength-dependent. Clouds are more absorptive at the longer wavelengths (Figure 2), where snow albedo is also lower (Figure 1a), so increasing cloud optical thickness τ_c causes the NIR snow albedo to increase (table 1).

Changes in spectrally-integrated snow albedo due to differential atmospheric absorption (the visible albedo is insensitive to τ_c .) will also be caused by changes in water vapor optical depth, τ_w , and the atmospheric path ($\sec \theta_0$, where θ_0 is the solar zenith angle). We hypothesize that the effects c , w , and $\sec \theta_0$ can be lumped together, so that only one predictor, t , is needed. This will be desirable not just for simplifying the parameterization, but because not all GCMs compute τ_c , but they all obtain t .

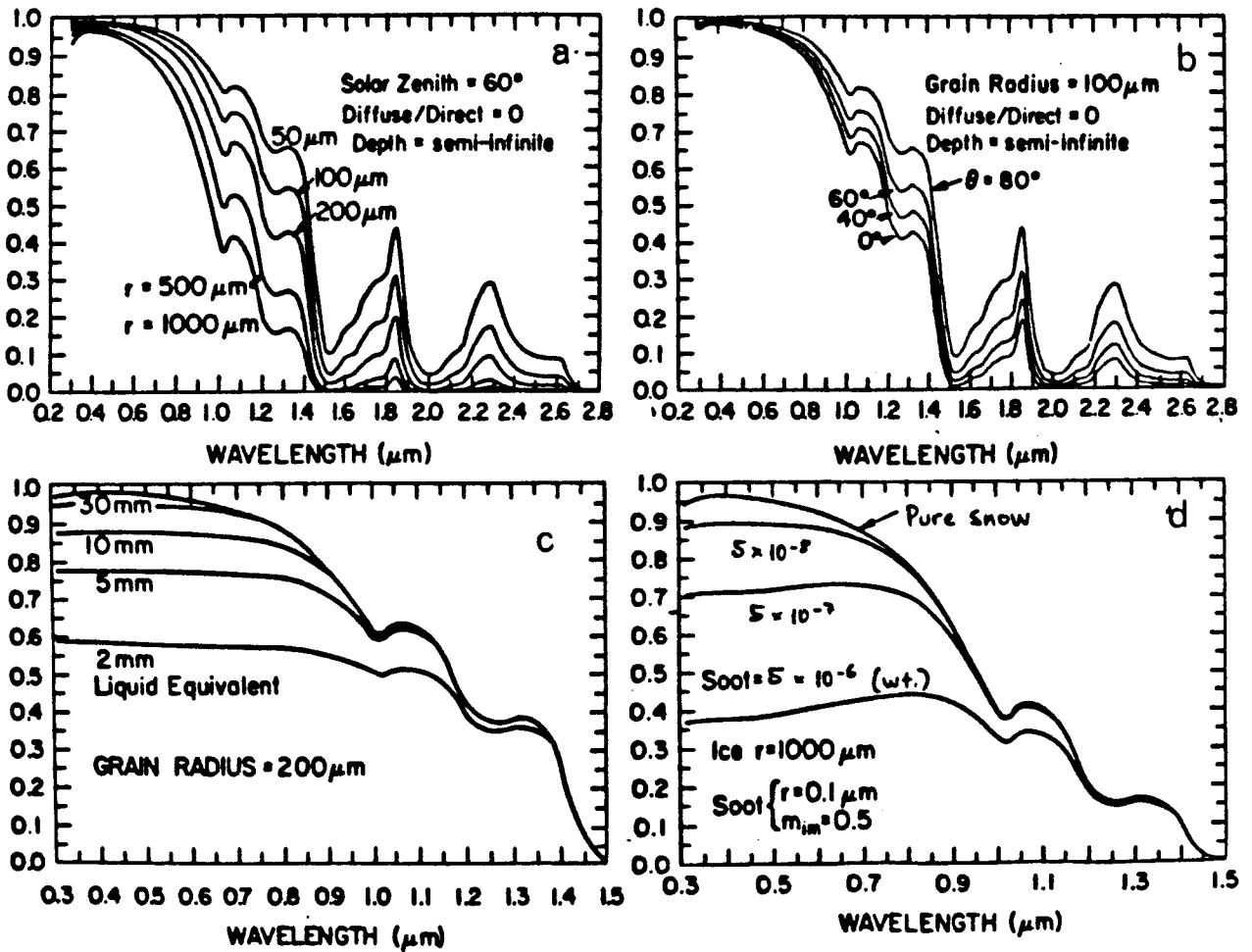


Fig. 1 Plots of the effects on the spectral albedo of snow of (a) snow grain size, (b) solar zentith angle, (c) snowpack thickness, and (d) contamination by soot (from WWI and WWII).

Table 1. Visible and near-infrared snow albedos for clear and cloudy Arctic sky conditions (using unusually thick cloud for Arctic; $\tau_c = 40$).

Spectral Interval (m)	Sky Condition	$\cos \theta_0$	Snow Albedo	Solar Downflux ($W m^{-2}$)
visible (0.3-0.7)	clear	0.40	0.98	226.5
visible (0.3-0.7)	cloud	0.40	0.97	171.7
infrared (0.7-3.0)	clear	0.40	0.64	195.3
infrared (0.7-3.0)	cloud	0.40	0.78	60.6

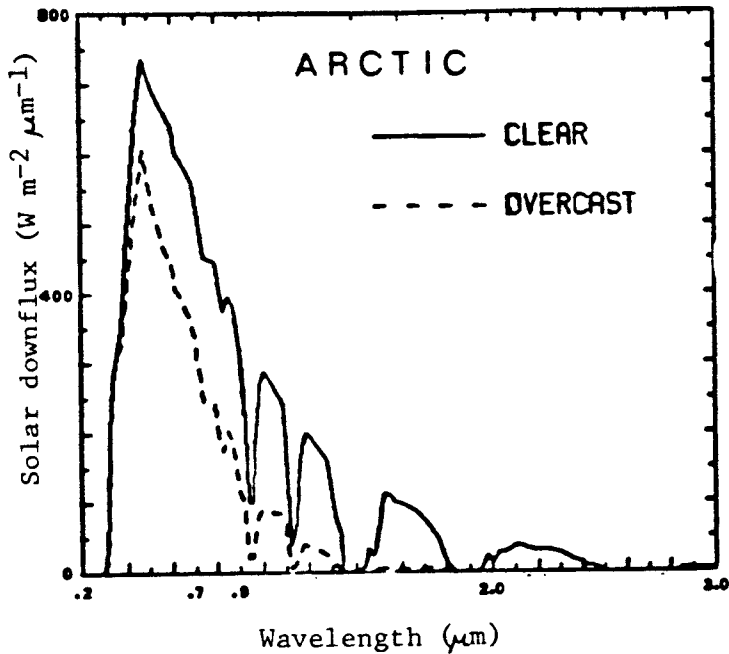


Fig. 2. Spectral distribution of incoming solar downflux ($\text{W m}^{-2} \mu\text{m}^{-1}$) for the Arctic summer under clear and cloudy (with an unusually thick cloud; optical thickness = 40) sky conditions. These are calculated using the ATRAD mode (Wiscombe *et al.*, 1984).

Table 2 shows the breakdown of the parameterization from (a) the final combination of visible and NIR albedos and downfluxes (F_{vis} , F_{nir}) into a single value of the snow albedo, to (d) the list of input values needed from the GCM to complete the parameterization. The parameterization will estimate the visible and NIR (clear-sky) snow albedos as functions of three main parameters: effective grain size, r , effective soot, s , and an effective zenith cosine, μ . The effect of cloud cover on the NIR snow albedo may be estimated using a value of the atmospheric transmittance, t .

The effective zenith cosine, μ , is a linear combination of the diffuse and direct-beam fractions of the solar irradiance and the diffuse and direct-beam zenith cosines (μ_d , μ_0). This relationship holds because the snow albedo is linear in μ for both the visible and NIR spectra. The fraction of insolation at the surface that is diffuse (d) will be parameterized, possibly as a combination of the atmospheric transmissivity and the direct-beam zenith angle. Because the spectral signatures of the grain radius and of the zenith angle are similar in their effect on the snow albedo, the two variables may be parameterized as one value, an effective grain size, r . Some properties of the albedo which may be useful are that it is nearly linear in $\cos \theta_0$, and that it is nearly linear in $r^{1/2}$ in the visible (Bohren and Barkstrom, 1974), but not in the NIR (WWI, figure 9).

The problem remains that snow grain size is difficult to predict, which is unfortunate since grain size is the most important variable controlling snow albedo. We will have to use observational data to develop a crude parameterization of grain size, probably in terms of the snow age and its temperature history, following the works of Anderson (1976).

Table 2. Parameterization for snow albedo α_s .

(a)	$\alpha_{tot} = \frac{F_{nir} \alpha_{nir} + F_{vis} \alpha_{vis}}{F_{nir} + F_{vis}}$
(b)	$\alpha_{vis} = f(r, s, \theta)$ $\alpha_{nir} = f(r, s, \theta) \text{ (clear)}$ $\alpha_{nir} = f(r, s, \theta, t) \text{ (cloudy)}$
(c)	effective grain size $r = f(\text{age, temperature})$ effective soot content $s = f(s, h, ua)$ effective zenith cosine $\mu = \cos \theta = d \mu_d + (1-d) \mu_0$, where $\mu_d = 0.65$. diffuse fraction $d = f(\theta_0, t)$ atmospheric transmittance $t = F(\text{surface}) / F(\text{top of the atmosphere})$
(d)	Need from GCM: temperature history, age of snow downward fluxes at surface, F_{vis} , F_{nir} solar zenith cosine μ_0 atmospheric transmittance $t = \frac{F(sfc)}{F(toa)}$. snow thickness ($g\text{ cm}^{-2}$) underlying albedo ua impurity content (as soot) s

Our work thus far has concentrated on how to lump together the soot content, snow thickness, and underlying albedo. Increasing soot concentrations in the snowpack and decreasing snow thickness lower integrated snow albedos (α_{vis} , α_{nir}) in a similar manner (figure 3), and might therefore be combined into one parameter, an effective soot concentration, s . For each snow albedo of one grain size and underlying surface albedo, there is associated one value of snow thickness, h ($g\text{ cm}^{-2}$), and one value of soot concentration, s (ppmw). Figure 4 shows the relationships between these values of soot and snow thickness. The regression lines plotted for these figures are for several combinations of α_s , r and ua . The fit of this relationship is improved by allowing the coefficients of the regression line to vary as functions of ua .

Figure 5 shows the errors involved in using an effective soot to calculate the integrated snow albedo. The parameterization shown in these figures breaks down for the case of an underlying surface albedo greater than the albedo of an optically-thick snow layer. A dirty snow layer covering a clean snowpack would be one example of this situation. An approach based on the underlying surface albedo, the snow thickness, and the snow grain radius, will be used to interpolate the snow albedo for the special case when ua is greater than α_s .

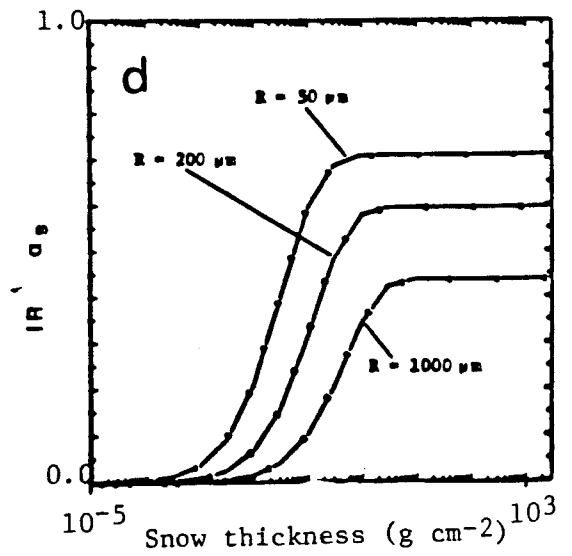
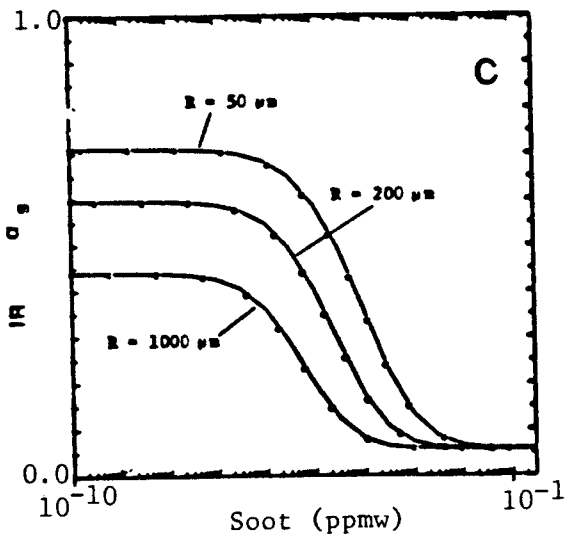
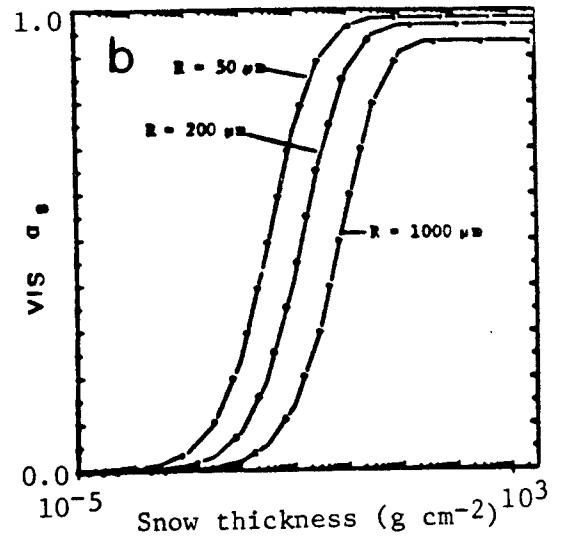
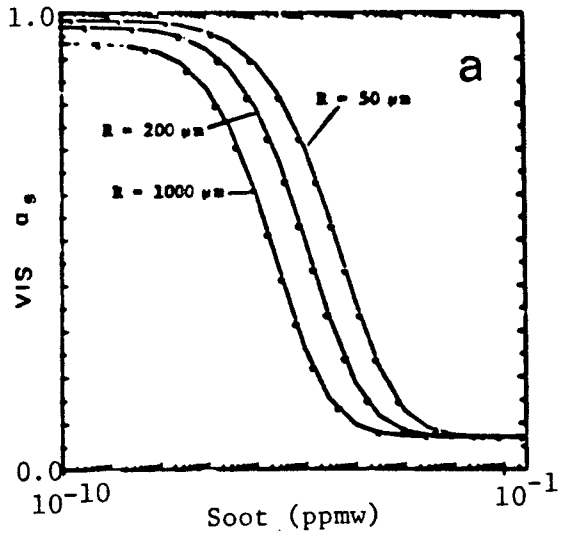


Fig. 3. Relationships between integrated snow albedo (α_s) and soot concentration in deep snow (a) and (c), and between integrated snow albedo and thickness of pure snow (b) and (d) for the visible and near-infrared wavebands, for three values of grain size, r .

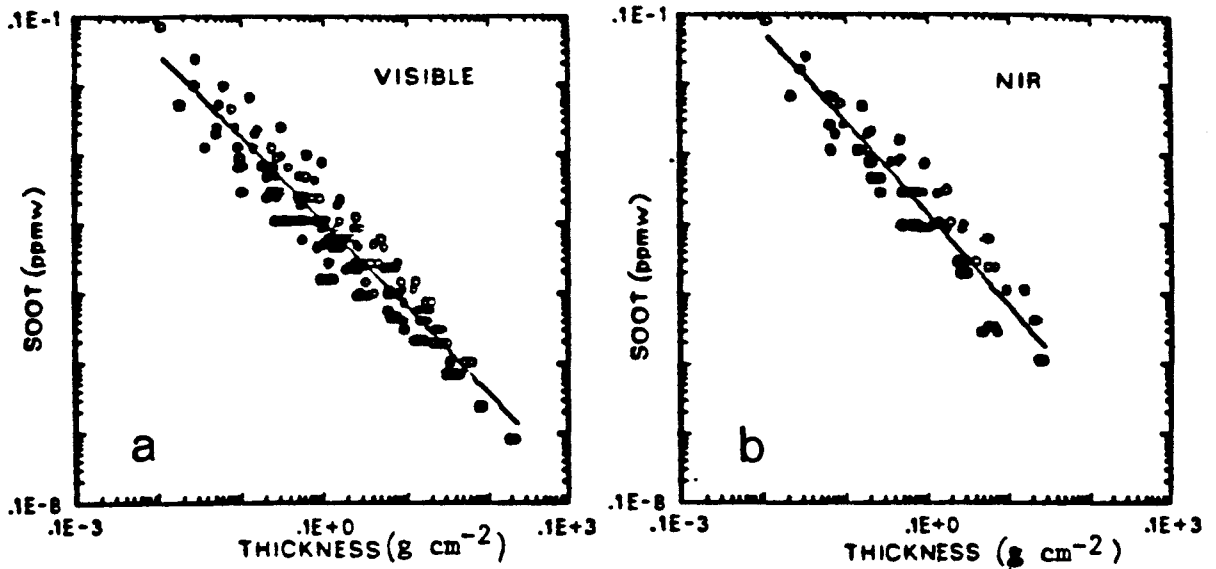


Fig. 4 A thin snowpack of pure snow has an albedo which can be mimicked by adding soot to a deep snowpack. These corresponding values of soot and thickness (for a variety of grain sizes and underlying albedos) are plotted as points here. The lines are least-squares fits, (a) visible (b) near-infrared.

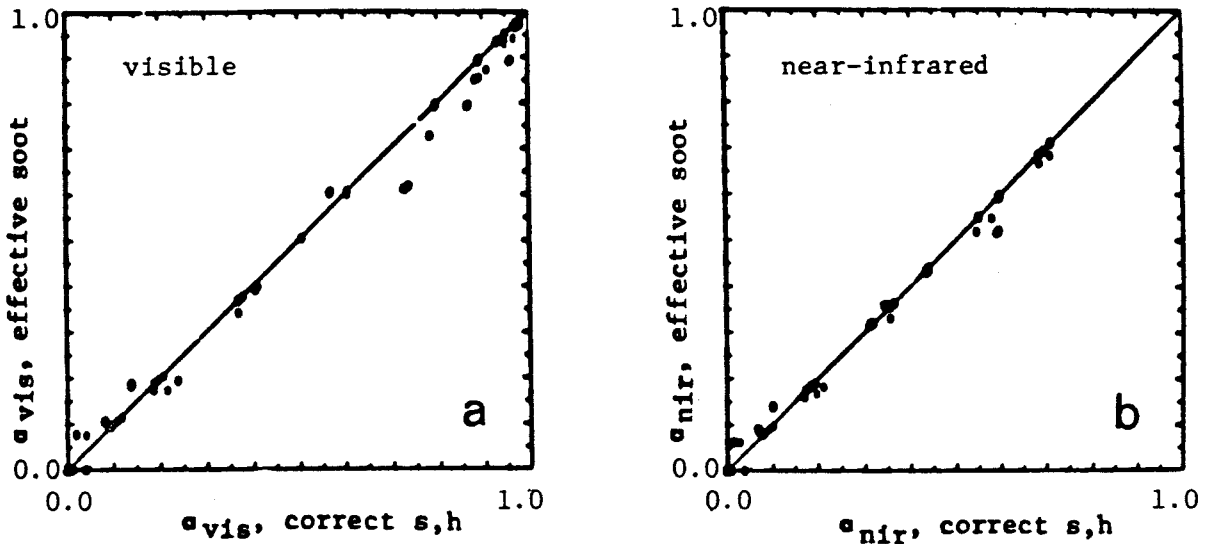


Fig. 5. Plots of integrated snow albedos using correct values of soot, s , and snow thickness, h , compared to integrated snow albedos using an "effective soot" calculation for (a) visible and (b) near-infrared integrations.

The final diagram (figure 6) outlines the structure we foresee for our parameterization. Task 1, the combination of snowpack thickness and concentration of soot into one parameter, an "effective soot", is now being completed. Task 2 involves the actual parameterization of the integrated snow albedos (visible and NIR) from given values of an effective grain radius, r , effective soot concentration, s , and effective zenith cosine, μ . The final task will then be to research methods by which the effective grain size can be estimated from data available to climate models. We are assuming that other steps not labelled as "tasks" will be relatively straight-forward.

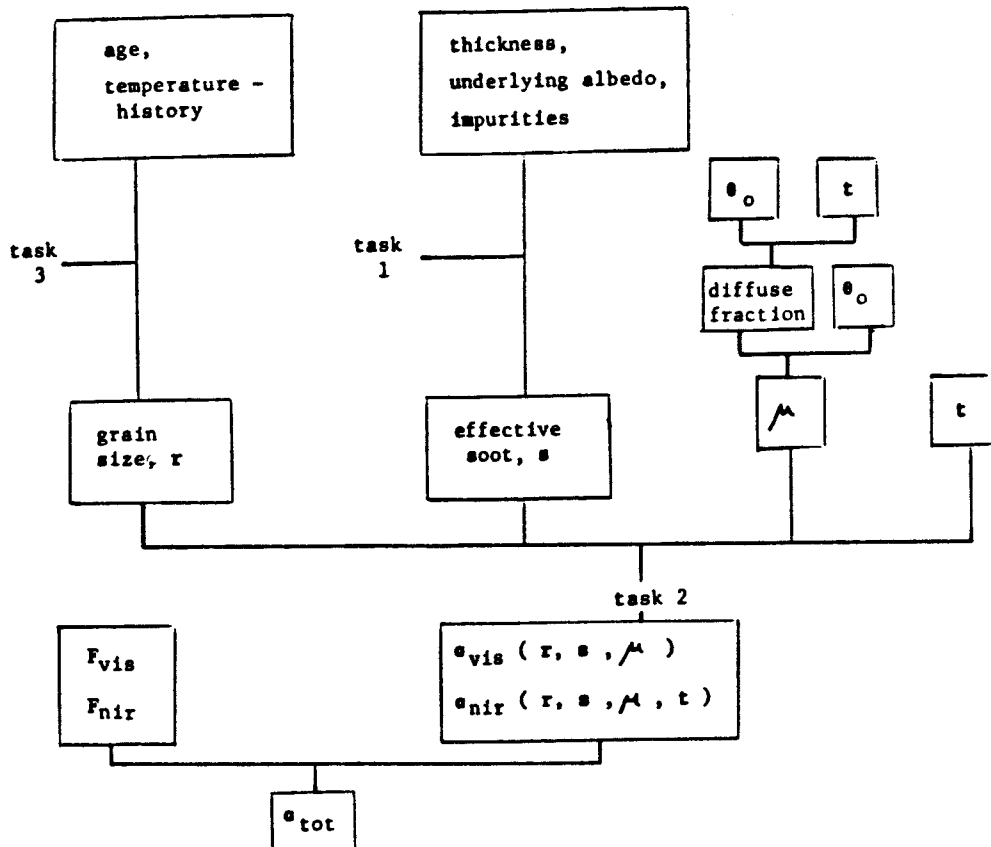


Fig. 6. Outline of research for parameterization of snow albedo.

This paper has presented completed work and outlined proposed tasks in the parameterization of snow surface albedo. Since much of this work is in the preliminary stages, the authors anticipate that changes will be made to the method as outlined at the workshop.

References

- Anderson, E.A. (1976) A Point Energy and Mass Balance Model of a Snow Cover. U.S. National Oceanic and Atmospheric Administration, Silver Spring, MD., NWS 19, 150p.
- Bohren, C.F.; Barkstrom, B.R. (1974) Theory of the optical properties of snow. Journal of Geophysical Research, v.79(30), p.4527-4535.
- Warren, S.G.; Wiscombe, W.J. (1980) A model for the spectral albedo of snow. II. Snow containing atmospheric aerosols. Journal of the Atmospheric Sciences, v.37, p.2734-2745.
- Wiscombe, W.J.; Warren, S.G. (1980) A model for the spectral albedo of snow. I. Pure snow. Journal of the Atmospheric Sciences, v.37, p.2712-2733.
- Wiscombe, W.J.; Welch, R.M.; Hall, W.D. (1984) The effects of very large drops on cloud absorption. Part I: Parcel models. Journal of the Atmospheric Sciences, v.41, p.1336-1355.

Acronyms

Atmospheric General Circulation Models

ECMWF	European Centre for Medium Range Weather Forecasting Bracknell, Berkshire, England.
GFDL	Geophysical Fluid Dynamics Laboratory Princeton, New Jersey
GISS	Goddard Institute for Space Studies New York, New York.
GLAS	Goddard Laboratory for Atmospheric Science Greenbelt, Maryland.
LMD	Laboratoire Meteorologie Dynamique Paris, France.
NCAR	National Center for Atmospheric Research Boulder, Colorado.
OSU	Oregon State University Corvallis, Oregon.
UKMO	United Kingdom Meteorological Office Bracknell, Berkshire, England